Radiology

Computer-aided US Diagnosis of Breast Lesions by Using Cell-based Contour Grouping[1]

Jie-Zhi Cheng, MS
Yi-Hong Chou, MD
Chiun-Sheng Huang, MD, PhD
Yeun-Chung Chang, MD, PhD
Chui-Mei Tiu, MD
Kuei-Wu Chen, MS
Chung-Ming Chen, PhD

Purpose: To develop a computer-aided diagnostic algorithm with automatic boundary delineation for differential diagnosis of benign and malignant breast lesions at ultrasonography (US) and investigate the effect of boundary quality on the performance of a computer-aided diagnostic algorithm.

Materials and Methods: This was an institutional review board–approved retrospective study with waiver of informed consent. A cell-based contour grouping (CBCG) segmentation algorithm was used to delineate the lesion boundaries automatically. Seven morphologic features were extracted. The classifier was a logistic regression function. Five hundred twenty breast US scans were obtained from 520 subjects (age range, 15–89 years), including 275 benign (mean size, 15 mm; range, 5–35 mm) and 245 malignant (mean size, 18 mm; range, 8–29 mm) lesions. The newly developed computer-aided diagnostic algorithm was evaluated on the basis of boundary quality and differentiation performance. The segmentation algorithms and features in two conventional computer-aided diagnostic algorithms were used for comparative study.

Results: The CBCG-generated boundaries were shown to be comparable with the manually delineated boundaries. The area under the receiver operating characteristic curve (AUC) and differentiation accuracy were 0.968 ± 0.010 and 93.1% ± 0.7, respectively, for all 520 breast lesions. At the 5% significance level, the newly developed algorithm was shown to be superior to the use of the boundaries and features of the two conventional computer-aided diagnostic algorithms in terms of AUC (0.974 ± 0.007 versus 0.890 ± 0.008 and 0.788 ± 0.024, respectively).

Conclusion: The newly developed computer-aided diagnostic algorithm that used a CBCG segmentation method to measure boundaries achieved a high differentiation performance.

Supplemental material: *http://radiology.rsna.org/lookup/suppl/doi:10.1148/radiol.09090001/-/DC1*

[1] From the Institute of Biomedical Engineering, College of Medicine, and College of Engineering, National Taiwan University, #1, Sec. 1, Jen-Ai Road, Taipei 100, Taiwan (J.Z.C., K.W.C., C.M.C.); Department of Radiology, Taipei Veterans General Hospital and National Yang Ming University, Taipei, Taiwan (Y.H.C., C.M.T.); and Departments of Surgery (C.S.H.) and Radiology and Medical Imaging (Y.C.C.), College of Medicine, National Taiwan University, Taipei, Taiwan.
Received January 15, 2009; revision requested February 17; revision received May 30; accepted June 30; final version accepted August 18. Supported by National Science Council, Taiwan, R.O.C. (grant 95-2221-E-002-023-MY3).
Address correspondence to C.M.C. (e-mail: *chung@ntu.edu.tw*).

Computer-aided diagnosis for breast ultrasonography (US) has been shown as promising to help with differential diagnosis of benign and malignant breast lesions (1–4). Not only does a computer-aided diagnostic system alone have the potential to achieve a reasonably high prediction rate (1,2) but the performance of human observers in interpretation of breast US may be improved with a computer-aided diagnostic system (3,4). Nevertheless, it remains impractical to use these computer-aided diagnostic algorithms in clinical applications. The primary difficulty lies in the extraction of robust mathematic features with high differentiating power.

Two types of mathematic features (regional and morphologic) have been proposed to model the US features. The regional features characterize the gray-scale and textural image properties of breast scans (eg, echogenicity and posterior acoustic shadowing). The morphologic features describe the shape and contour of breast lesions.

Most previous computer-aided diagnostic algorithms for breast lesions shown at US are designed on the basis of the regional features, such as run-length (5,6), Markovian (5,6), co-occurrence matrix (7), posterior acoustic attenuation pattern (6,8), or autocorrelation (8,9) features. Nevertheless, many regional features have the potential drawback of setting dependence, since the value of a regional feature may vary with the parameter setting of the US imaging system for the same scanning view of a person.

However, morphologic features tend to be more robust to the variation of parameter settings than regional features and have been shown to be effective because the shape and contour of a breast lesion usually do not change dramatically with the parameter settings (1,2,8,10,11). However, extraction of morphologic features relies on a reasonably good boundary delineation of the breast lesion, which is generally a difficult task in practice, owing to the irregular shape of the breast lesions, as well as the speckle, tissue-related textures, and artifacts seen on breast US scans.

Important as it is, effective boundary delineation of breast lesions on US scans has not received proportional attention in the development of computer-aided diagnostic algorithms. Breast lesion boundaries have been mostly extracted by using such conventional approaches as threshold level setting (1,8), deformable models (3,12), and level-set methods (2) in the previous computer-aided diagnostic algorithms by using morphologic features. Although satisfactory performances have been attained for the image sets used in these studies, each algorithm has deficiencies in dealing with the complex shapes and texture patterns within and surrounding the lesions, in general.

Our study aim was to develop a computer-aided diagnostic algorithm with automatic boundary delineation for differential diagnosis of benign and malignant breast lesions at US.

Advances in Knowledge

- Cell-based contour grouping (CBCG) is an effective approach for automatic delineation of the lesion boundaries with more than 80% of the CBCG-generated boundaries having the smaller computer-observer distances than the interobserver distances.
- The quality of computer-generated boundaries, which is shown to be a significant linear covariate ($P < .001$), is important for the classification performance of a computer-aided diagnostic algorithm.

Materials and Methods

Study Subjects and Image Acquisition

For performance evaluation and comparison, 520 breast US scans obtained from 520 subjects were retrospectively and randomly selected from the database of breast US scans at Taipei Veterans General Hospital (Taipei, Taiwan). The sample population may be considered as representative of the females in Taiwan who choose to have the breast checkup and treatment in a medical center. The sample size of 520 was determined on the basis of a pilot study (13) that used 71 US scans, which were randomly sampled from the same database but completely different from the 520 US scans used in this study. The null hypothesis was that the distance between the boundaries generated by the newly developed segmentation algorithm was larger than the maximum interobserver distance. With Type I error and power set to .005 and .95, respectively, the results of the power analysis of the pilot study suggested that the required sample size was 171 for the worst case. Taking into account the possibility that a segmentation algorithm might fail in finding a closed lesion boundary, the sample size for this study was determined to be about three times that of the sample size of 520 lesions, as suggested by the pilot study.

These 520 images were acquired from 1996 to 2004 by using US scanners (HDI 3000 and HDI 5000; Advanced Technology Laboratories, Bothell, Wash) equipped with broadband transducers

Implication for Patient Care

- Computer-aided diagnosis of breast cancers may be improved by using the CBCG segmentation algorithm and morphologic features.

Published online
10.1148/radiol.09090001

Radiology 2010; 255:746–754

Abbreviations
AUC = area under the receiver operating characteristic curve
CBCG = cell-based contour grouping
ROI = region of interest

Author contributions:
Guarantors of integrity of entire study, J.Z.C., C.M.C.; study concepts/study design or data acquisition or data analysis/interpretation, all authors; manuscript drafting or manuscript revision for important intellectual content, all authors; approval of final version of submitted manuscript, all authors; literature research, J.Z.C., Y.H.C., Y.C.C., C.M.T., K.W.C., C.M.C.; clinical studies, Y.H.C., C.S.H., C.M.T.; experimental studies, J.Z.C., K.W.C., C.M.C.; statistical analysis, J.Z.C., K.W.C., C.M.C.; and manuscript editing, J.Z.C., Y.H.C., Y.C.C., C.M.T., C.M.C.

Authors stated no financial relationship to disclose.

(L10–5 and L12–5; Advanced Technology Laboratories). The institutional review board agreed that the patients' images could be used for study without written consent if their privacy was well protected. To ensure patient privacy, identifiers were removed from the images and data. There were 275 benign and 245 malignant cases (Table 1). All breast lesions were histopathologically proved by means of mastectomy (performed for malignant lesions that were surgically biopsied after US-guided metallic wire localization), US-guided core needle biopsy, or fine-needle aspiration cytologic analysis. The subject ages ranged from 15 to 89 years (mean age, 46 years ± 12 [standard deviation]). The mean values and ranges of the lesion sizes and the ages of patients in the benign and malignant groups were listed in Table 2.

Boundary Delineation

To delineate the breast lesion boundaries automatically and ensure the determined boundaries on the visually perceivable edges, a cell-based contour grouping (CBCG) algorithm was proposed for segmentation of US breast lesions as a two-level cell-based perceptual organization process. At the first level, the CBCG algorithm separated the region of interest (ROI) in prominent components, the boundaries of which were all visually perceivable edges and formed a superset of the desired lesion boundary. A prominent component was a contiguous region with a visually perceivable boundary, which might be a noise, an artifact, a substructure of a tissue, or a part of a breast lesion. The prominent components were identified by the cell competition algorithm (13). At the second level, the lesion boundary was sought by grouping the edges of the prominent components by using the cell-based graph search algorithm. The contour grouping process was achieved by converting the edges of the prominent components to a graph and using the depth-first-search algorithm incorporating Gestalt principles (14) to find the sequence of edges corresponding to the lesion boundary. As a result, five lesion boundaries were suggested on the basis of five cost functions. Details of this approach are given in Appendix E1 (online) and graphically shown in Figures 1 and 2.

Table 1

Tumor Types Involved in this Study

Lesion Type	No. of Tumors	Tumor Size (mm)
Benign		
Fibroadenoma	234	5–35 (16 ± 5)*
Echogenic cyst (including clustered microcysts)	23	5–24 (13 ± 4)*
Papilloma	10	6–13 (8 ± 2)*
Lobular fibrosis or focal fibrosis	4	11–20 (14 ± 4)*
Fat necrosis	2	13, 26
Intramammary lymph node	1	9
Neuroma	1	20
Malignant		
Infiltrative ductal carcinoma	212	8–29 (18 ± 6)*
Invasive lobular carcinoma	12	12–25 (20 ± 6)*
Colloid carcinoma	8	16–22 (19 ± 3)*
Ductal carcinoma in situ with microinvasion	6	10–25 (21 ± 5)*
Medullary carcinoma	3	10–20 (15 ± 3)*
Invasive papillary carcinoma	2	13, 22
Ductal carcinoma in situ	2	8, 12

* Data are the range; the means ± standard deviations are in parentheses.

Table 2

Lesion Size and Patient Age

Type and No. of Lesions	Tumor Size (mm)*	Age (y)*
Benign		
Group of 324 (n = 173)	5–35 (16.3 ± 6.2)	27–69 (43.7 ± 14.5)
Group of 196 (n = 102)	8–26 (15.6 ± 9.8)	15–59 (43.2 ± 14.1)
Group of 520 (n = 275)	5–35 (16.2 ± 7.9)	15–69 (44.5 ± 15.3)
Malignant		
Group of 324 (n = 151)	8–29 (16.5 ± 6.1)	38–66 (50.3 ± 10.1)
Group of 196 (n = 94)	10–27 (18.4 ± 9.0)	34–89 (52.3 ± 13.5)
Group of 520 (n = 245)	8–29 (16.7 ± 7.5)	34–89 (50.9 ± 11.4)

Note.—The group of 520 lesions is the entire set, the group of 324 lesions is the subset for performance comparisons among different algorithms, and the group of 196 lesions is the subset for which the segmentation method of the first algorithm cannot find closed lesion boundaries.

* Data are the range; the means ± standard deviations are in parentheses.

Features and Differentiation Method

The mathematic features used in the newly developed computer-aided diagnostic algorithm were seven morphologic features extracted from the automatically delineated lesion boundaries. These seven features were defined in our previous work (10), which included the number of substantial protuberances and depressions, lobulation index, elliptic-normalized circumference, elliptic-normalized skeleton, long-axis–to–short-axis ratio, depth-to-width ratio, and size of the lesion. The differentiation method was a logistic regression function (15); for each test data set, forward selection (16) was performed to select a set of features that yielded the best differentiation accuracy given the corresponding training data.

Performance Analysis and Evaluation

To quantify the quality of the lesion boundaries determined by using the

Figure 1

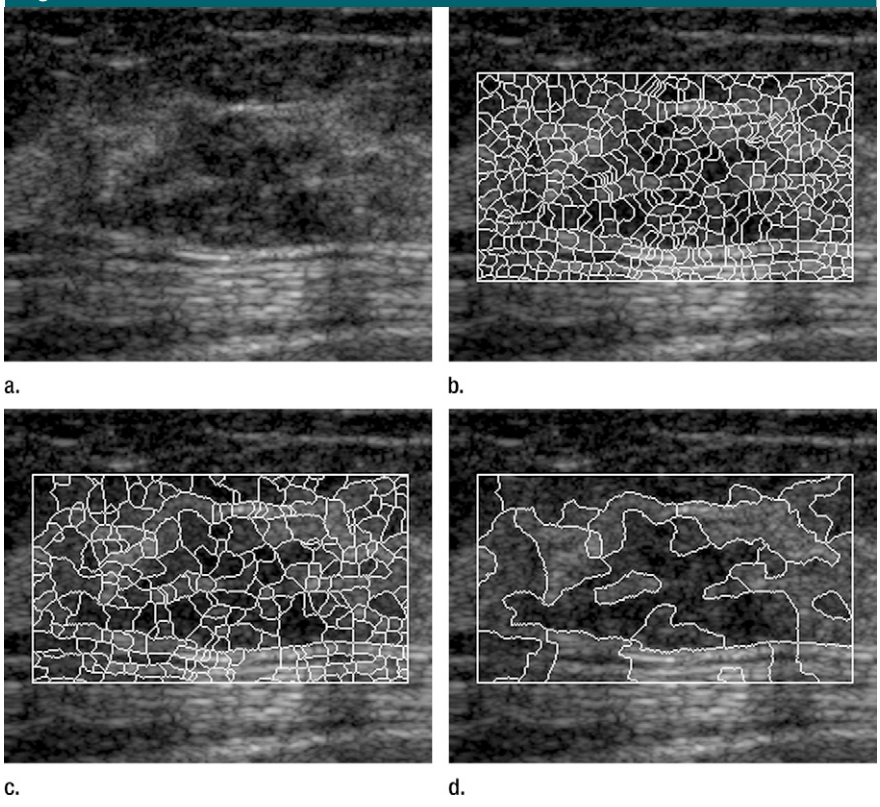

Figure 1: US performed in 43-year-old woman with cell competition algorithms shows **(a)** ROI of breast, **(b)** elementary cells obtained at first-pass watershed transformation process, **(c)** cells obtained at second-pass watershed transformation process, and **(d)** prominent components.

CBCG algorithm, each lesion was manually delineated by four graduate students (all nonauthors) studying medical image analysis and who had been trained to identify the lesion boundaries. The boundaries demarcated by these students were confirmed to be acceptable by four doctors experienced in breast US (one breast surgeon [C.S.H.] and three radiologists [Y.H.C., Y.C.C., and C.M.T.], each with 10–28 years experience). Each graduate student also determined computer-generated lesion boundaries by using the CBCG algorithm. For most US scans, each student only needed to choose an ROI. For less than 2% of 520 lesions, the students overcame the problem of ill-defined boundary by lowering the default threshold level value (T_2) for cell generation (Appendix E1 [online]). All 520 images were randomized to minimize potential bias on image type before they were presented to each student.

The quality of the lesion boundaries demarcated by an automatic segmentation algorithm was quantified by the percentage statistic PC_k for each computer-generated boundary set, where k = 1–4. The percentage statistic PC_k was defined as the mean percentage that the computer-to-observer distances

Figure 2

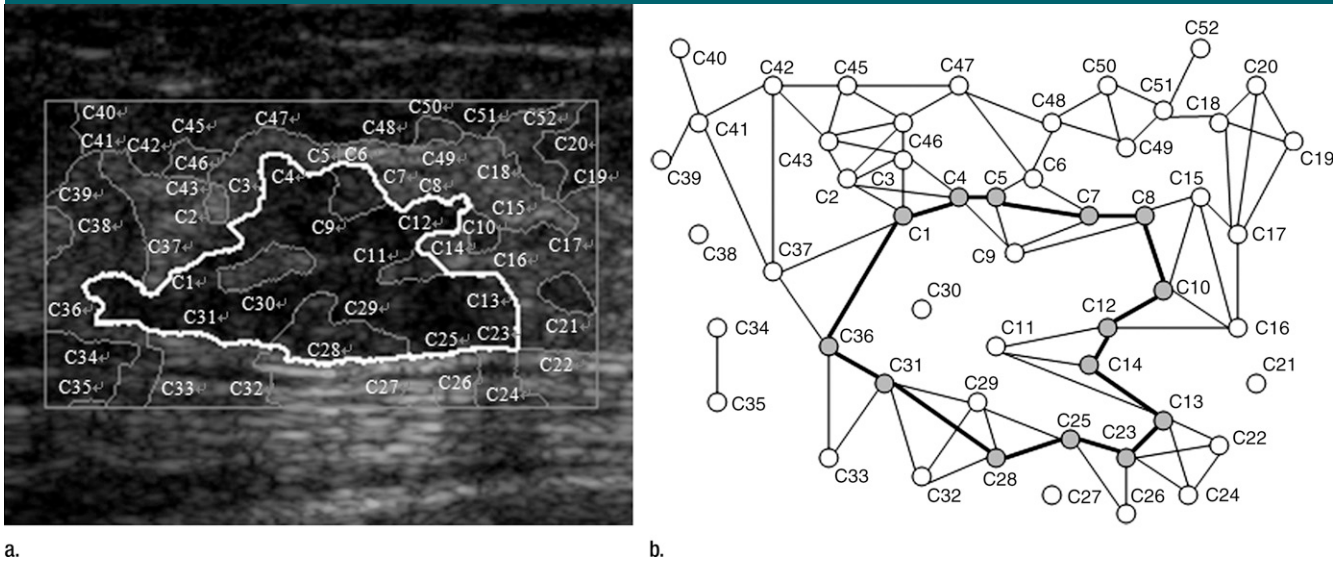

Figure 2: CBCG algorithms show **(a)** labeling of all 52 cell edges in Figure 1d, where thick edges defined lesion boundary, and **(b)** c-graph constructed from **a**, where gray nodes connected by thick links indicated one possible path sought by depth-first search on c-graph.

associated with the computer-generated boundaries (C_k) were less than or equal to the corresponding maximum interobserver distances. The detailed definition of percentage statistic PC_k is given in Appendix E1 (online).

The differentiation performance for each set of computer-generated boundaries was estimated on the basis of a 10-fold cross-validation. Six performance figures were reported. The first was the mean of the areas under the receiver operating characteristic curve (AUCs), calculated by using the four sets of computer-generated boundaries. The other five were the mean values of the best differentiation accuracies, as well as those of the sensitivities, specificities, and positive and negative predictive values defined at the best differentiation accuracies. A true-positive result was defined as a true malignant breast lesion that had been predicted to be malignant.

To examine the effect of boundary and feature sets on differentiation performance, the segmentation algorithms and feature sets of two conventional computer-aided diagnostic algorithms (1,2) developed mainly on the basis of morphologic features were implemented. The first computer-aided diagnostic algorithm (1) used a threshold level–based approach for boundary delineation, comprising five major steps, including median filtering, unsharp masking, contrast material enhancement, binary threshold level setting, and edge detection. The features were spiculation, ellipsoid shape, branch pattern, number of lobulations, and brightness of nodule. The second computer-aided diagnostic algorithm (2) used a level-set–based segmentation approach composed of four major steps, including anisotropic diffusion filtering, stick method, automatic threshold level setting, and level-set method. The features were form factor, roundness, aspect ratio, convexity, solidity, and extent.

The graduate students also determined lesion boundaries by using the segmentation methods in first and second computer-aided diagnostic algorithms for each breast US scan. The students needed to choose ROIs and were allowed to freely adjust all parameters and threshold levels involved in both algorithms to optimize the segmentation results. The default values were set as suggested by the first and second computer-aided diagnostic algorithms.

For each lesion, the features sets used in three computer-aided diagnostic algorithms were extracted from the boundary determined by using each of the three segmentation methods. It gave nine feature vectors for classification, each for a combination of boundary and feature set. To control the effect of the classifier on the differentiation performance, the same classifier (ie, the logistic regression function) with forward selection was used for each of the nine combinations.

The effect of boundary and feature sets on differentiation performances were analyzed on the basis of those lesions for which the segmentation methods in all three computer-aided diagnostic algorithms could determine closed boundaries. Consequently, only 324 of 520 breast lesions were used, including 199 benign and 125 malignant lesions. The other 196 lesions could not be demarcated successfully with closed boundaries by using the segmentation method used in the first algorithm. Table 2 summarizes the statistics for the lesion sizes and ages of the benign and malignant cases in different subsets, including the group of 324 (the subset for performance comparisons among different algorithms) and the group of 196 (the subset for which the segmentation method in the first algorithm cannot establish closed lesion boundaries) lesions. Comparisons for the lesion sizes and age distributions among different subsets were performed by using two-tailed two-sample Student *t* tests. To determine whether the 324 CBCG-generated boundaries were a reasonable representative subset of the 520 CBCG-generated boundaries in terms of boundary quality and differentiation performance, two-tailed paired-sample *t* tests were performed for the quality index and the AUCs for the 324 and 520 CBCG-generated boundaries in combination with the Chen feature.

The quality of the boundaries determined by using three segmentation algorithms was compared by using two-tailed paired-sample *t* tests given the percentage statistic PC_k. Three tests were performed for analysis and comparison of the differentiation performances of these nine combinations. First, two-tailed paired-sample *t* tests were performed to compare the differentiation performances achieved by three combinations given by three computer-aided diagnostic algorithms.

Two multivariate analyses were used to analyze the factors determining the differentiation performance for these nine combinations. The first analysis was a two-way within-subject analysis of variance with two categoric factors, boundary and feature set, from each of the computer-aided diagnostic programs. Two-tailed paired-sample *t* tests were performed for post hoc tests. The second analysis was a one-way within-subject analysis of variance performed with a covariate. The factor in this analysis was the feature set and the covariate was the boundary quality characterized by the percentage statistic PC_k. The dependent variables were the AUCs for both multivariate analyses. While the first analysis was performed to determine the importance of the boundary sets and feature sets, the second analysis further demonstrated the contribution of the boundary quality to the differentiation performance. Both multivariate analyses and all two-tailed paired-sample *t* tests were performed by using software (SPSS for Windows, version 16; SPSS, Chicago, Ill). A *P* value of .05 was considered to indicate a significant difference.

Results

No significant differences were found between the groups of 324 and 196 lesions in tumor sizes and age distributions by using two-tailed two-sample *t* tests at the 5% significance level. For the benign lesion comparisons, $P = .517$ for lesion size and $P = .78$ for age between both groups. For malignant lesion comparisons, $P = .089$ for lesion size and P = .218 for age between both

groups. In comparing the sizes of the benign and malignant lesions for the groups of 520 and 324 lesions, $P = .461$ and .195, respectively, which suggested that there were no significant differences between the benign and malignant lesion sizes in both groups.

The newly developed computer-aided diagnostic algorithm was evaluated in terms of the boundary quality and the differentiation performance by using 10-fold cross-validation. Each of the four students was able to determine closed lesion boundaries for all breast US scans by using the newly developed CBCG algorithm, which resulted in four sets of lesion boundaries, each containing 520 CBCG-generated boundaries. The mean distance between the manually delineated and CBCG-generated boundaries was 3.4 pixels. The mean of the maximum interobserver distance was 4.7 pixels (Appendix E1 [online]). The mean percentage statistic PC_k of these four sets of 520 CBCG-generated boundaries was 82.69% ± 0.90. An example of different CBCG-generated boundaries is shown in Figure 3.

The differentiation performance achieved by using the newly developed algorithm for 520 breast US scans is given in Table 3. Additionally, by adjusting the threshold level for the output values of the classifier, the sensitivities increased to 98.4% and 100% while the mean specificities decreased to 84.1% and 60.0%.

For performance analysis and comparison, the mean values of the percentage statistic PC_k for the CBCG-generated boundaries and the first and second computer-aided diagnostic algorithms were 82.93% ± 1.10, 65.63% ± 3.51, and 26.72% ± 1.55, respectively (Fig 4). Two-tailed paired-sample t test results showed that the boundary quality achieved by using the CBCG algorithm was better than that achieved by using the segmentation method in the first ($P < .002$) and second ($P < .001$) computer-aided diagnostic algorithms, in terms of the percentage statistics.

The sensitivities for the newly developed computer-aided diagnostic algorithm for 324 breast US scans, increased to 98.4% and 100% while the mean specificities decreased to 76.5% and 65.7%.

To test whether the 324 CBCG-generated boundaries were a reasonable representative subset of the 520 CBCG-generated boundaries, two-tailed paired-sample t tests were performed on the percentage statistic PC_k and the AUCs calculated by using the Chen function. $P = .178$ for comparing the percentage statistic PC_k and $P = .25$ (both $> .05$) for comparing AUCs, which suggested that the four sets of 324 CBCG-generated boundaries had comparable boundary quality and differentiation performance to the four sets of 520 CBCG-generated boundaries.

To compare the differentiation performances achieved by the combinations of boundary and feature set, as defined by three computer-aided diagnostic algorithms, the AUCs of the three

Figure 3

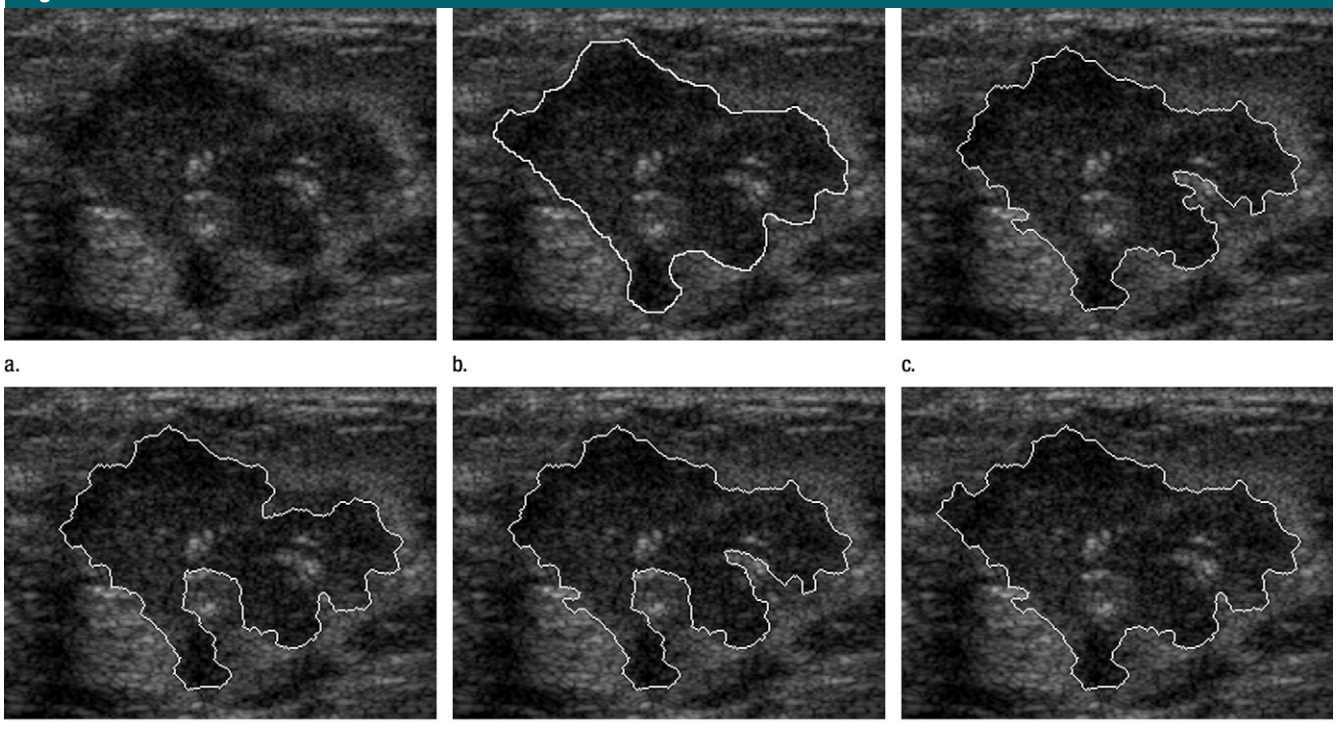

Figure 3: Breast US performed in 44-year-old woman of boundaries generated manually and by using CBCG algorithm shows **(a)** malignant lesion in center, **(b)** one of four manual boundaries for lesion, and **(c–f)** four CBCG-generated boundaries generated by using five cost functions (C1–C5). C4 and C5 produced exact same boundary (**f**).

Table 3

Differentiation Performances Measured by Using 10-fold Cross-validation

Boundary	Feature	AUC	Accuracy (%)	Sensitivity (%)	Specificity (%)	Positive Predictive Value (%)	Negative Predictive Value (%)
CBCG (n = 520)	Chen	0.968 ± 0.010	93.1 ± 0.7	96.9 ± 1.2	89.8 ± 1.7	89.5 ± 1.6	97.0 ± 1.0
CBCG	Chen	0.974 ± 0.007	92.7 ± 0.5	90.4 ± 3.1	94.1 ± 2.3	90.8 ± 3.0	94.1 ± 1.7
CBCG	First CAD	0.959 ± 0.010	91.3 ± 1.6	86.8 ± 5.0	94.1 ± 3.6	90.6 ± 5.4	92.0 ± 2.5
CBCG	Second CAD	0.929 ± 0.014	88.4 ± 1.2	83.0 ± 5.0	91.7 ± 2.5	86.5 ± 3.1	89.7 ± 2.7
First CAD	Chen	0.899 ± 0.013	85.3 ± 1.0	79.6 ± 2.0	88.8 ± 1.5	81.8 ± 1.9	87.4 ± 1.1
First CAD	First CAD	0.890 ± 0.008	83.0 ± 1.7	75.6 ± 4.2	87.7 ± 3.5	79.7 ± 4.0	85.2 ± 1.9
First CAD	Second CAD	0.892 ± 0.012	85.3 ± 1.0	80.0 ± 2.4	88.5 ± 1.3	81.5 ± 1.6	87.6 ± 1.3
Second CAD	Chen	0.792 ± 0.035	77.3 ± 2.1	71.4 ± 8.8	81.0 ± 5.6	70.7 ± 3.9	82.1 ± 3.6
Second CAD	First CAD	0.781 ± 0.030	74.3 ± 2.7	56.0 ± 8.9	85.8 ± 1.8	71.1 ± 2.1	75.8 ± 3.5
Second CAD	Second CAD	0.788 ± 0.024	77.0 ± 2.5	68.6 ± 5.7	82.3 ± 3.4	71.0 ± 3.6	80.7 ± 2.8

Note.—Data are the mean ± standard deviation. CAD = computer-aided diagnostic algorithm.

combinations showed that all $P < .005$. The AUC results suggested that with a logistic regression function as the classifier, the newly developed computer-aided diagnostic algorithm could achieve better differentiation performance than could the boundaries and features defined by using the first and second computer-aided diagnostic algorithms.

A two-way within-subject analysis of variance showed that the factor and boundary had a significant effect on the differentiation performance ($P < .001$), but the effect of the factor *feature set* was not significant ($P = .09$). The interaction between boundary and feature set was not significant ($P = .12$). Subsequent post hoc tests on the different levels of the factor *boundary* revealed that the differentiation performance achieved with CBCG-generated boundaries was significantly better than those with the boundaries calculated with the segmentation method in the first ($P < .001$) and second ($P < .001$) computer-aided diagnostic algorithms. A one-way within-subject analysis of variance performed with a covariate further showed that boundary quality was a significant linear covariate ($P < .001$), while the factor *feature set* had no significant effect on the differentiation performance ($P = .257$).

Figure 4

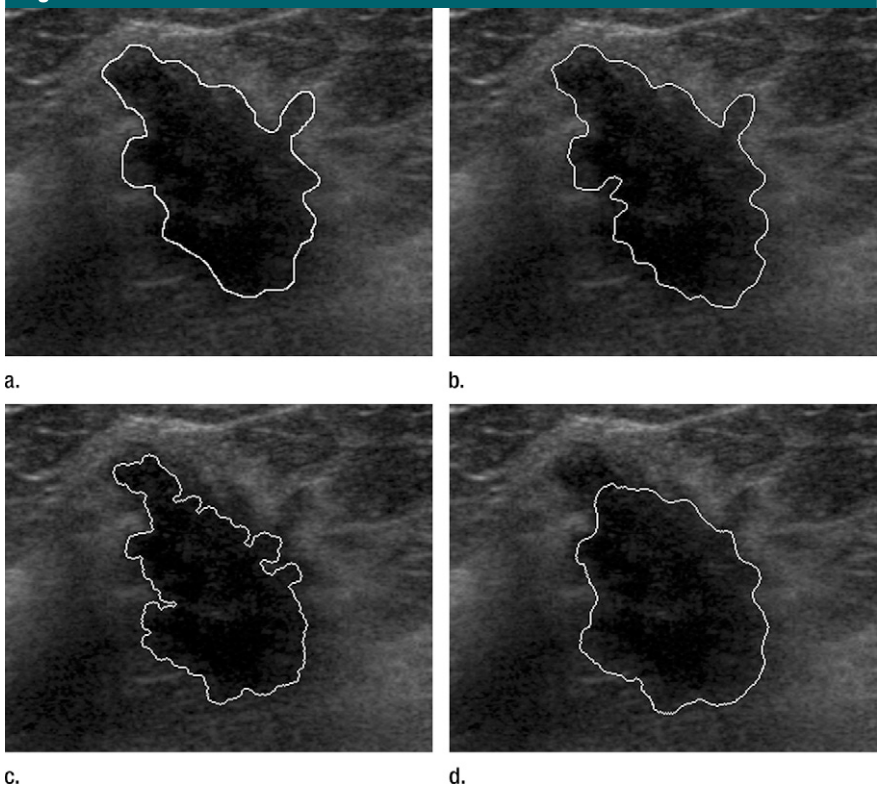

Figure 4: Breast US performed in 76-year-old woman shows **(a)** manually delineated boundary for malignant lesion, **(b)** CBCG-generated boundary, **(c)** boundary generated by using segmentation method in first algorithm, and **(d)** boundary generated by using segmentation method in second computer-aided diagnostic algorithm.

Discussion

Morphologic features are known to be effective (1,2,8,10,11) in computer-aided differentiation of benign and malignant breast lesions on US scans, various ones of which have been proposed to characterize the malignancy of the US breast lesions. However, the effectiveness of these features depends highly on the quality of the determined lesion boundaries. We present an efficient computer-aided diagnostic algorithm with an automatic segmentation approach. Not only were the lesion boundaries determined by using the

CBCG algorithms shown to be close to the manually delineated boundaries, but the morphologic features extracted from these CBCG-generated boundaries gave a high differentiation performance.

Corroborated by the reasonably high percentage statistics (>80%) for both the entire set and a subset of 520 breast lesions, the CBCG-generated boundaries seemed comparable with the manually delineated boundaries. The high quality of the CBCG-generated boundaries might be attributed to the idea of grouping cell edges in lesion boundaries, the advantages of which are twofold. First, the cell edges are coincident with the visually perceivable edges. Second, the search space formed by the cell edges is much smaller, more manageable, and thus more likely to help find the optimal solution of the lesion boundaries than the search space constituted by the pixels in the ROI.

By using the Chen morphologic features (10) extracted from the CBCG-generated boundaries, the newly developed computer-aided diagnostic algorithm attained high differentiation performances for both the entire set and a subset of the 520 breast lesions. They were comparable with other studies on observers' performances, given the observed US features. For instance, the respective sensitivity and specificity reported by Stavros et al (17) were 98.4% and 67.8%; those reported by Skaane and Engedal (18) were 99.5% and 29%. They were also comparable with the computer-aided diagnostic performances given the features extracted from the manually delineated boundaries. For example, the AUCs calculated by Chen et al (10) and Chou et al (11) were 0.959 and 0.970, respectively.

The boundary quality achieved by using the CBCG algorithm was shown to be better than that attained by using the segmentation method in two conventional computer-aided diagnostic algorithms. One common deficiency of these segmentation algorithms was their inability to capture weak edges owing to similar acoustic impedance or inhomogeneous fields (eg, shadowing). Moreover, neither of the segmentation algorithms assured that the determined boundaries coincided with visually perceivable edges. As a consequence, the threshold level–based segmentation method in the first algorithm was not able to find the closed boundaries for 196 of 520 breast lesions, even when the operators were allowed to freely adjust the values of the parameters inherent in the algorithm. Use of the level-set method in the second computer-aided diagnostic algorithm frequently required a compromise between how close the zero level-set was to the desired boundary and leakage from the weak edges.

The differentiation performance of the newly developed computer-aided diagnostic algorithm was shown to be better than those attained by using the boundaries and feature sets from the two conventional algorithms (1,2). Our analysis showed that the main factor for determining the differentiation performances was the boundary rather than the feature set, which is reasonable because a computer-generated boundary with a better quality (ie, a higher percentage statistic in this study) implies a greater resemblance to the manually delineated boundaries and thus serves as a better representative of the true lesion boundary.

One limitation of this study was the inference to the importance of the boundary quality that was made on the basis of only three sets of boundaries generated by using three segmentation algorithms. Further investigation with more segmentation algorithms involved would be required to achieve a more robust inference. Another limitation was that only boundary sets, boundary quality, and feature sets have been considered in the multivariate analyses. Theoretically, differentiation performance may also be affected by such factors as lesion size, US image quality, and how well defined the lesion boundary is in a breast US scan. Although the boundary quality may account for the net effect of these factors on a segmentation algorithm, it deserves a more thorough study with a larger sample size to take into account various factors. The third limitation was that only two conventional computer-aided diagnostic algorithms have been implemented for performance comparison and analysis, though not many computer-aided diagnostic algorithms based on morphologic features have been previously developed.

In conclusion, a computer-aided diagnostic algorithm with an automatic CBCG segmentation algorithm was proposed in this paper to help diagnose breast lesions on US scans. The high differentiation performance achieved by the newly developed computer-aided diagnostic algorithm was primarily a result of the effective features and the high-quality computer-generated lesion boundaries. The CBCG-generated boundaries were not only coincident with visually perceivable edges theoretically, but were also shown to be comparable with the manually delineated boundaries. The boundary quality of the CBCG algorithm was shown to be better than those achieved by the segmentation methods of the two conventional algorithms (1,2). By using the same classifier, the differentiation performance of the newly developed computer-aided diagnostic algorithm was shown to be better than those attained by using the boundaries and features of the two conventional algorithms. Given two multivariate analyses, the boundary quality was identified as a crucial factor in determining the differentiation performance.

References

1. Joo S, Yang YS, Moon WK, Kim HC. Computer-aided diagnosis of solid breast nodules: use of an artificial neural network based on multiple sonographic features. IEEE Trans Med Imaging 2004;23(10):1292–1300.
2. Chang RF, Wu WJ, Moon WK, Chen DR. Automatic ultrasound segmentation and morphology based diagnosis of solid breast tumors. Breast Cancer Res Treat 2005;89(2):179–185.
3. Sahiner B, Chan HP, Roubidoux MA, et al. Malignant and benign breast masses on 3D US volumetric images: effect of computer-aided diagnosis on radiologist accuracy. Radiology 2007;242(3):716–724.
4. Horsch K, Giger ML, Vyborny CJ, Venta LA. Performance of computer-aided diagnosis in

the interpretation of lesions on breast sonography. Acad Radiol 2004;29(2):157–164.

5. Goldberg V, Manduca A, Ewert DL, Gisvold JJ, Greenleaf JF. Improvement in specificity of ultrasonography for diagnosis of breast tumors by means of artificial intelligenc. Med Phys 1992;19(6):1475–1481.
6. Zheng Y, Greenleaf JF, Gisvold JJ. Reduction of breast biospies with a modified self-organizing map. IEEE Trans Neural Netw 1997;8(6):1386–1396.
7. Garra BS, Krasner BH, Horii SC, Ascher S, Mun SK, Zeman RK. Improving the distinction between benign and malignant breast lesions: the value of sonographic texture analysis. Ultrason Imaging 1993;15(4):267–285.
8. Horsch K, Giger ML, Venta LA, Vyborny CJ. Computerized diagnosis of breast lesions on ultrasound. Med Phys 2002;29(2):157–164.
9. Chang RF, Wu WJ, Moon WK, Chen DR. Improvement in breast tumor discrimination by support vector machines and speckle-emphasis texture analysis. Ultrasound Med Biol 2003;29(5):679–686.
10. Chen CM, Chou YH, Han KC, et al. Breast lesions on sonograms: computer-aided diagnosis with nearly setting-independent features and artificial neural networks. Radiology 2003;226(2):504–514.
11. Chou YH, Tiu CM, Hung GS, Wu SC, Chang TY, Chiang HK. Stepwise logistic regression analysis of tumor contour features for breast ultrasound diagnosis. Ultrasound Med Biol 2001;27(11):1493–1498.
12. Chen DR, Chang RF, Wu WJ, Moon MK, Wu WL. 3-D breast ultrasound segmentation using active contour model. Ultrasound Med Biol 2003;29(7):1017–1026.
13. Chen CM, Chou YH, Chen CS, et al. Cell-competition algorithm: a new segmentation algorithm for multiple objects with irregular boundaries in ultrasound images. Ultrasound Med Biol 2005;31(12):1647–1664.
14. Koffka K. Principles of Gestalt psychology. New York, NY: Harcourt Brace & World, 1935.
15. Dillon WR, Goldstein M. Multivariate analysis: method and applications. New York, NY: Wiley, 1984.
16. He DC, Wang L, Guibert J. Texture discrimination based on an optimal utilization of texture features. Pattern Recognit 1988;21(2):141–146.
17. Stavros AT, Thickman D, Rapp CL, Dennis MA, Parker SH, Sisney GA. Solid breast nodules: use of sonography to distinguish between benign and malignant lesions. Radiology 1995;196(1):123–134.
18. Skaane P, Engedal K. Analysis of sonographic features in the differentiation of fibroadenoma and invasive ductal carcinoma. AJR Am J Roentgenol 1998;170(1):109–114.
19. Vincent L, Soille P. Watershed in digital spaces: an efficient algorithm based on immersion simulations. IEEE Trans PAMI 1991;13(6):583–597.
20. Cheng JZ. Cell-based image segmentation for 2D and 2D series ultrasound images [master's thesis]. Taipei, Taiwan: National Taiwan University, 2007.
21. Chalana V, Linker DT, Haynor DR, Kim Y. A multiple active contour model for cardiac boundary detection on echocardiographic sequences. IEEE Trans Med Imaging 1996; 15(3):290–298.